# Sensitivity of Structural Demand to Ground Motion Selection and Modification Methods


**C. Cantagallo, G. Camata & E. Spacone**
*University "G. D'Annunzio" of Chieti-Pescara, Italy*

**SUMMARY:**
The use of Non-Linear Dynamic Analyses provides significant uncertainties on the seismic demand, especially when real records are used. As these uncertainties strongly depend on the Ground Motion Selection and Modification (GMSM) methods, the spectrum-compatibility criterion and the method based on the minimization of the scaling factor are compared in this work. The variability of the engineering demand parameter obtained by subjecting ten reinforced concrete structures to different groups of records is studied through a sensitivity analysis called "*Tornado Diagram Analysis*". The analyses results show that the variability of the structural demand produced by the variation of the ground motion profile is significantly amplified with the increase in the complexity and the irregularity of the structures. More specifically, for regular structures, the selected GMSM criteria provide very similar variability while with the increase of irregularities, the spectrum-compatibility criterion produces a minimization of the demand uncertainty.

*Keywords: sensitivity analysis, ground motion selection and scaling criteria, nonlinear dynamic analysis*

## 1. INTRODUCTION

As Non-Linear Time History Analyses (NLTHA) become more prevalent in practice, there is the need to better understand how the selection and modification of real records influences the structural demand. Currently, there are many ground motion selection and modification (GMSM) methods available for dynamic analyses. Unfortunately, there is no consensus yet concerning the accuracy and precision of these methods. Recent works (Porter et al., 2002; Lee and Mosalam, 2005; Faggella et al., 2012) show that among all sources of uncertainty deriving from material properties (concrete, steel and supporting soil), design assumptions and earthquake-induced ground motion, the latter shows to be the most unpredictable and variable. The record selection and modification process should minimize the variability induced by the records on the structural demand as uncertainties in the seismic demand vary significantly depending on the selected GMSM method used, and a higher uncertainty increases the capacity that must be designed into the system. The objective of this work is to investigate the selection and scaling criteria of real records which produce the lowest variability in the structural demand. To this purpose two different GMSM methods are compared by evaluating the variability of the corresponding structural demand through a deterministic sensitivity analysis of the first order called "*Tornado Diagram Analysis*" (Porter et al., 2002). This analysis shows the effect of input variable uncertainties on the output variability.

## 2. STRUCTURAL MODELS

In order to investigate the record selection and scaling criteria which produces the lowest variability in the structural demand, ten tri-dimensional MDOF reinforced concrete structures, with an increasing degree of complexity and irregularity, are examined. More specifically, the first nine structures (Structures 1-9) are designed to capture all the most important structural responses, while Structure 10

represents a typical example of an existing structure. Figure 2.1 shows the structural configuration and the principal modelling features of each analyzed structure.

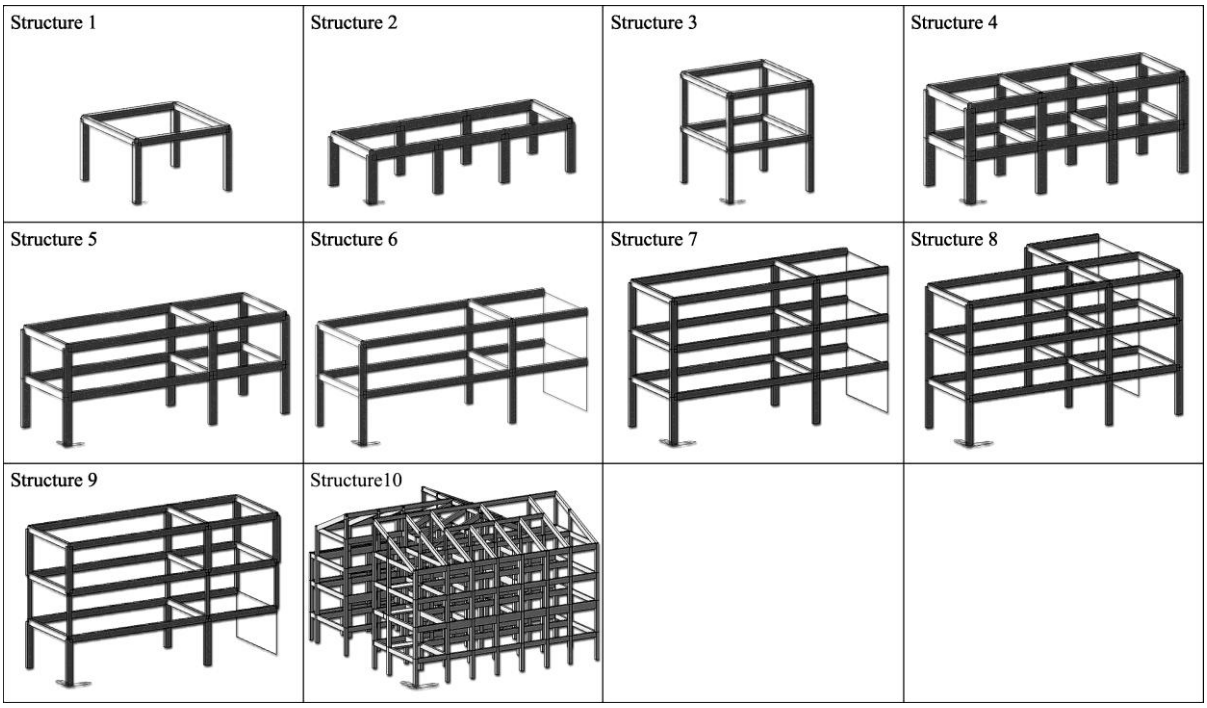


**Figure 2.1.** Reinforced concrete frame structures

The non-linear dynamic analyses are performed with the commercial computer software Midas Gen 7.21 (Midas, 2007) using a force-based fiber beam model (Spacone et al., 1996). In all structures, floor rigid diaphragms are used. The concrete and steel non-linear behaviour are modelled respectively with the Kent and Park (1971) and the Menegotto and Pinto (1973) constitutive laws. For all structures, except Structure 10, columns are modelled with forced-based fiber elements, while beams and walls with linear elastic elements. Because of its irregularity and complexity, in Structure 10 both beams and columns are modelled with fiber models. The non-linear modelling of elements is performed by using four Gauss-Lobatto integration points. The geometrical, mechanical and dynamic properties of the ten analyzed RC frame structures are briefly summarized in Table 2.1 and Table 2.2.

**Table 2.1.** Principal geometrical and mechanical properties of the analyzed structures

| Structure | | | Columns | | |
|---|---|---|---|---|---|
| Structure n. | Max Height (m) | Max Plan Dimensions (m) | Column Section | Column Concrete Fibers (n.) | Column Steel Rebar (n. and diameter) |
| Structure 1 | 3.0 | 5x5 | 30x30 | 10x10 ($f_c$ = 20 *MPa*) | 4Φ12 ($f_y$ = 430 *MPa*) |
| Structure 2 | 3.0 | 15x5 | 30x60 | 6x12 ($f_c$ = 20 *MPa*) | 4Φ14 ($f_y$ = 430 *MPa*) |
| Structure 3 | 6.0 | 5x5 | 30x30 | 10x10 ($f_c$ = 20 *MPa*) | 4Φ12 ($f_y$ = 430 *MPa*) |
| Structure 4 | 6.0 | 15x5 | 30x60 | 6x12 ($f_c$ = 20 *MPa*) | 4Φ14 ($f_y$ = 430 *MPa*) |
| Structure 5 | 6.0 | 15x5 | 20x50 | 4x10 ($f_c$ = 20 *MPa*) | 4Φ10 ($f_y$ = 430 *MPa*) |
| Structure 6 | 6.0 | 15x5 | 20x40 | 4x8 ($f_c$ = 20 *MPa*) | 4Φ10 ($f_y$ = 215 *MPa*) |
| Structure 7 | 9.0 | 15x5 | 20x40 | 4x8 ($f_c$ = 20 *MPa*) | 4Φ10 ($f_y$ = 430 *MPa*) |
| Structure 8 | 9.0 | 15x10 | 20x40 | 4x8 ($f_c$ = 20 *MPa*) | 4Φ10 ($f_y$ = 215 *MPa*) |
| Structure 9 | 9.0 | 15x5 | 20x40<br>20x20 | 4x8 ($f_c$ = 20 *MPa*)<br>4x4 ($f_c$ = 20 *MPa*) | 4Φ10 ($f_y$ = 375 *MPa*)<br>4Φ10 ($f_y$ = 375 *MPa*) |
| Structure 10 | 16.3 | 26x26 | 45x40<br>40x50<br>50x40<br>30x30 | 8x7 ($f_c$ = 16.5 *MPa*)<br>5x10 ($f_c$ = 16.5 *MPa*)<br>6x12 ($f_c$ = 16.5 *MPa*)<br>6x6 ($f_c$ = 16.5 *MPa*) | 4Φ18 ($f_y$ = 375 *MPa*)<br>4Φ18 ($f_y$ = 375 *MPa*)<br>4Φ18 ($f_y$ = 375 *MPa*)<br>4Φ14 ($f_y$ = 375 *MPa*) |

**Table 2.2.** Elastic translational periods, modal participation masses and modal participation factors of the ten analyzed structures

| Structure | Elastic translational Periods | | Modal Participation Masses | | | | Modal Participation factors - Γ | |
|---|---|---|---|---|---|---|---|---|
| | $T_1$ | $T_2$ | Mode 1 | | Mode 2 | | Mode 1 | Mode 2 |
| n. | (sec) | (sec) | X-dir | Y-dir | X-dir | Y-dir | $\Gamma_1$ | $\Gamma_2$ |
| Structure 1 | 0.17 | 0.17 | 100% | 100% | 100% | 100% | 1.000 | 1.00 |
| Structure 2 | 0.16 | 0.11 | 0.00 | 100.0 | 0.00 | 0.00 | 1.000 | 1.00 |
| Structure 3 | 0.41 | 0.41 | 66.9% | 22.2% | 22.2% | 66.9% | 1.147 | 1.147 |
| Structure 4 | 0.29 | 0.18 | 0.00 | 91.9% | 89.6% | 0.00 | 1.153 | 1.157 |
| Structure 5 | 0.44 | 0.23 | 0.00 | 80.6% | 87.5% | 0.00 | 1.199 | 1.217 |
| Structure 6 | 0.52 | 0.43 | 0.00 | 55.0% | 86.7% | 0.00 | 1.228 | 1.232 |
| Structure 7 | 0.92 | 0.86 | 0.00 | 51.1% | 85.0% | 0.00 | 1.160 | 1.173 |
| Structure 8 | 0.90 | 0.76 | 12.9% | 36.9% | 73.1% | 6.7% | 1.126 | 1.151 |
| Structure 9 | 0.67 | 0.61 | 0.00 | 51.2% | 76.9% | 0.00 | 1.258 | 1.248 |
| Structure 10 | 0.90 | 0.75 | 0.1% | 82.3% | 81.7% | 0.1% | 1.300 | 1.303 |

In order to investigate the GMSM method producing the lowest variability in the structural demand, a single Engineering Demand Parameter (EDP), the Maximum Interstory Drift Ratio MIDR, is considered. MIDR is computed as the maximum percentage interstory drift DXY over time (the record duration), that is MIDR = max|DXY(*t*)|. For each record, the interstory drift ratio at an instant *t* is computed as:

$$\mathrm{DXY}\ t = \sqrt{\mathrm{DX}\ t^{\,2} + \mathrm{DY}\ t^{\,2}} \tag{2.1}$$

where DX(*t*) and DY(*t*) are the instantaneous interstory drifts in the X and Y directions, respectively, between the centers of mass of two adjacent floors.

## 3. RECORD SELECTION AND MODIFICATION

The record selection is based on the Probabilistic Seismic Hazard Analysis (PSHA) derived from an Italian study carried out by the National Institute of Geophysics and Volcanology (INGV) and the Civil Protection Department (DPC). This work (*http://esse1.mi.ingv.it/*) provides the PSHA and the disaggregation for each point of a regular grid covering the entire Italian territory. Records are selected using an earthquake scenario with moment magnitude $M_w$, epicentral distance R and class soil A. The reference site is located on rock soil in Sulmona (AQ-Italy) - 42.084° latitude and 13.962° longitude -. The $M_w$-R bins providing the larger contribution to the seismic hazard at a specified probability of exceedance (Spallarossa and Barani, 2007) are derived from the seismic hazard disaggregation (Bazzurro and Cornell, 1999). The target scenario examined in this work corresponds to a probability of exceedance of 10% in 50 years and it is characterized by $M_w$ between 5.5 and 6.5 and R between 15 and 30 km. Epicentral distances smaller than 15 km are not considered to avoid "near-field" effects. Based on this earthquake scenario, 61 ground motion records (each consisting of two orthogonal horizontal components) are selected from two databases: the European Strong-motion Database (ESD) and the ITalian ACcelerometric Archive (ITACA). The ground motion components of these records are correlated since they are recorded along random directions and not normally oriented along the ground motion principal directions (Penzien and Watabe, 1975). Therefore, in order to align each ground motion along its principal directions, all 61 selected records are uncorrelated using a coordinate transformation (Lopez et al., 2004).

Following a previous study by Cantagallo et al. (2012), the spectra corresponding to the 61 selected records are scaled to the target spectral acceleration $S_a(T^*)$ corresponding to the "non-linear period" $T^*$. Cantagallo et al. (2012) show that $T^*$ considers the elongation of the effective structural period during the non-linear analysis. The paper also reveals that $S_a(T^*)$ is well correlated with the deformation demand (expressed in Cantagallo et al. 2012 by the MIDR) and it produces the lowest variability in

structural demand among intensity measures investigated. The "non-linear period" $T^*$ represents the period corresponding to the initial branch of the bilinear idealized capacity curve obtained from the non-linear static (pushover) analysis, according to the Eurocode 8 (UNI EN 1998-1:2005: Annex B). In general, the $T^*$ values vary depending on the distribution of lateral loads and the loading direction, but in this study only the $T^*$ values corresponding to the "uniform" pattern applied in the direction of the first linear translational period are used to obtain the scaling factors.

For each record and for any structural period $T$, a single spectral acceleration $S_a(T)$ is obtained as a geometric mean of the two corresponding horizontal spectral components. As stated in Beyer and Bommer (2006), the geometric mean is the most widely used definition of the horizontal component of motion (Beyer and Bommer, 2006). A single spectrum is therefore computed from the geometric mean of the spectral values of the X and Y components. More specifically, the spectral acceleration corresponding to the period $T^*$ is defined by Eq. 3.1, through which a single scale factor for both accelerograms corresponding to the horizontal components of each record can be performed:

$$S_a\ T^* = \sqrt{S_{a\mathrm{X}}\ T^* \cdot S_{a\mathrm{Y}}\ T^*} \tag{3.1}$$

The 61 pre-selected spectra are then scaled so that each $S_a(T^*)$ is equal to the corresponding target spectral acceleration derived from the PSHA. Subsequently, three different groups of 20 records are selected, called respectively "Comb. 1", "Comb. 2" and "Comb. 3". More specifically, the records belonging to Comb. 1 are those with the lowest scaling factor, while the records belonging to Comb. 2 and Comb. 3 are selected according to a spectrum-compatibility criterion so that, in the spectrum-compatibility range (equal to $0.2T^*$-$2T^*$), the mean elastic spectrum calculated from all time histories is between 90% and 110% of the uniform hazard spectrum. Since the spectrum-compatible records may consist of ground motions with very different characteristics, two groups of spectrum-compatible records are considered (Comb. 2 and Comb. 3). The spectrum-compatibility criterion used for Comb. 2 and Comb. 3 differs from that provided by the Eurocode 8 – Part 1 (UNI EN 1998-1:2005), which states that

- recorded accelerograms have to be scaled to the value of $a_gS$ for the zone under consideration (without explaining if this should be done for uni-directional analysis only or for bi-directional analysis too);
- in the range of periods $0{,}2T_1$ - $2T_1$, where $T_1$ is the fundamental period of the structure, no value of the elastic spectrum calculated from all time histories should be less than 90% of the corresponding value elastic response spectrum (no spectrum-compatibility upper limit is established).

Table 3.1 describes, for each combination and structure, the maximum, minimum and average values of the Scale Factors SF, Peak Ground Accelerations PGA and corresponding standard deviations $\sigma_{SF}$ and $\sigma_{PGA}$.

**Table 3.1.** $T^*$ values obtained at the ULS from the pushover analyses applying to each structure a distribution of lateral loads proportional to a "uniform" and "modal" pattern

| ***Structure*** | ***Comb.*** | $\mathbf{SF_{max}}$ | $\mathbf{SF_{min}}$ | $\mathbf{SF_{mean}}$ | $\boldsymbol{\sigma_{SF}}$ | $\mathbf{PGA_{max}}$ | $\mathbf{PGA_{min}}$ | $\mathbf{PGA_{mean}}$ | $\boldsymbol{\sigma_{PGA}}$ |
|---|---|---|---|---|---|---|---|---|---|
| Structure 1 | **Comb. 1** | 3.73 | 0.58 | 2.30 | 0.98 | 4.39 | 1.80 | 2.93 | 0.76 |
| | **Comb. 2** | 6.54 | 0.59 | 3.52 | 1.61 | 3.88 | 1.80 | 2.64 | 0.59 |
| | **Comb. 3** | 8.27 | 0.59 | 3.56 | 1.95 | 3.88 | 1.80 | 2.63 | 0.60 |
| Structure 2 | **Comb. 1** | 4.53 | 0.76 | 2.80 | 1.19 | 7.79 | 1.87 | 3.73 | 1.66 |
| | **Comb. 2** | 9.52 | 0.76 | 4.61 | 2.87 | 4.56 | 1.25 | 2.73 | 0.82 |
| | **Comb. 3** | 8.98 | 0.76 | 4.27 | 2.33 | 4.56 | 1.25 | 2.78 | 0.81 |
| Structure 3 | **Comb. 1** | 4.76 | 1.07 | 2.97 | 1.09 | 7.88 | 1.49 | 3.72 | 1.62 |
| | **Comb. 2** | 8.87 | 1.77 | 4.82 | 2.32 | 4.58 | 1.27 | 2.71 | 1.02 |
| | **Comb. 3** | 8.43 | 1.19 | 4.24 | 2.02 | 4.82 | 1.27 | 2.89 | 1.09 |
| Structure 4 | **Comb. 1** | 4.76 | 1.07 | 2.97 | 1.09 | 7.88 | 1.49 | 3.72 | 1.62 |
| | **Comb. 2** | 8.87 | 1.77 | 4.82 | 2.32 | 4.58 | 1.27 | 2.71 | 1.02 |
| | **Comb. 3** | 8.43 | 1.19 | 4.24 | 2.02 | 4.82 | 1.27 | 2.89 | 1.09 |
| Structure 5 | **Comb. 1** | 5.29 | 1.03 | 3.27 | 1.21 | 11.64 | 1.53 | 4.09 | 2.96 |
| | **Comb. 2** | 9.68 | 1.03 | 5.24 | 2.75 | 6.94 | 1.49 | 3.18 | 1.64 |

| | | | | | | | | | |
|---|---|---|---|---|---|---|---|---|---|
| | **Comb. 3** | 9.68 | 1.03 | 5.37 | 2.61 | 6.94 | 1.49 | 3.11 | 1.70 |
| Structure 6 | **Comb. 1** | 4.77 | 1.27 | 2.92 | 1.07 | 7.18 | 1.25 | 3.59 | 1.86 |
| | **Comb. 2** | 8.52 | 1.27 | 4.41 | 2.32 | 4.79 | 1.25 | 2.61 | 1.04 |
| | **Comb. 3** | 8.52 | 1.27 | 4.55 | 2.18 | 5.12 | 1.25 | 2.84 | 1.16 |
| Structure 7 | **Comb. 1** | 5.29 | 1.03 | 3.27 | 1.21 | 11.64 | 1.53 | 4.09 | 2.96 |
| | **Comb. 2** | 9.68 | 1.03 | 5.24 | 2.75 | 6.94 | 1.49 | 3.18 | 1.64 |
| | **Comb. 3** | 9.68 | 1.03 | 5.37 | 2.61 | 6.94 | 1.49 | 3.11 | 1.70 |
| Structure 8 | **Comb. 1** | 4.57 | 1.14 | 3.03 | 0.96 | 8.37 | 1.35 | 3.72 | 2.26 |
| | **Comb. 2** | 9.70 | 1.14 | 4.88 | 2.72 | 5.51 | 1.35 | 2.98 | 1.31 |
| | **Comb. 3** | 11.70 | 1.14 | 5.21 | 2.98 | 5.51 | 1.35 | 2.78 | 1.30 |
| Structure 9 | **Comb. 1** | 4.65 | 1.24 | 2.92 | 0.97 | 6.93 | 1.37 | 3.47 | 1.85 |
| | **Comb. 2** | 9.85 | 1.24 | 4.89 | 2.69 | 5.94 | 1.37 | 2.79 | 1.24 |
| | **Comb. 3** | 9.85 | 1.24 | 5.03 | 2.70 | 5.94 | 1.37 | 2.77 | 1.32 |
| Structure 10 | **Comb. 1** | 12.19 | 0.40 | 3.60 | 3.30 | 10.18 | 1.32 | 3.43 | 2.26 |
| | **Comb. 2** | 9.40 | 0.99 | 5.07 | 2.71 | 7.37 | 1.32 | 3.00 | 1.53 |
| | **Comb. 3** | 9.40 | 0.99 | 5.50 | 2.52 | 7.37 | 1.32 | 3.06 | 1.75 |

## 4. PROPAGATION OF UNCERTAITIES IN THE SEISMIC DEMAND

The degree of uncertainty of the seismic demand is strictly connected to the uncertainty inherent to the input variables such as earthquake ground motion, geometry, mechanical properties of resisting components and models adopted for simulating the structural behavior. Sensitivity studies are used to identify the input variables that mostly affect the uncertainty in the seismic demand. A sensitivity analysis investigates the variation (uncertainty) of the output in relation to different sources of variation of the input. Over the years many types of sensitivity analyses were developed for various disciplines and only recently they have been applied in earthquake engineering. The "*Tornado diagram analysis*" is a first order sensitivity analysis which draws its origin from decision analyses (Eschenbach, 1992). It consists of a set of horizontal bars, one for each random input variable, whose lengths represent the variation of the EDP due to each considered input variable (Figure 4.1).

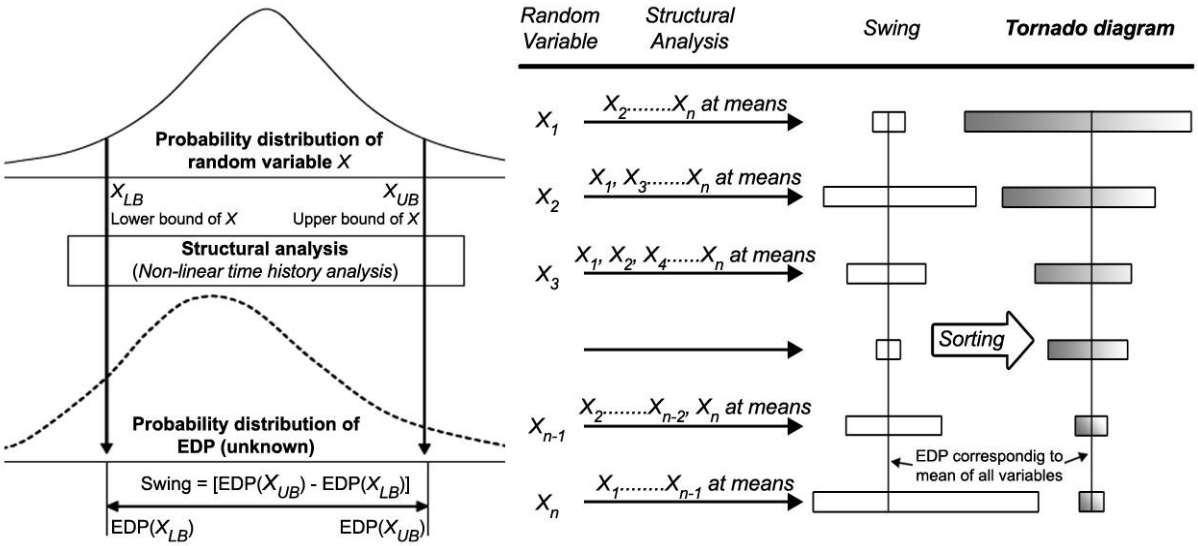


**Figure 4.1.** Procedure for obtaining the Tornado diagram: on the left summary scheme for developing a single swing and on the right outline of the general method (adapted from Binici and Mosalam, 2007)

To obtain a Tornado diagram, the selection of a set of input variables and the construction of the corresponding probability distribution functions is performed. Subsequently, each input variable is set to its median value (50$^{th}$ percentile), and the output is measured, establishing in this way a baseline output. One by one, each input parameter is fixed to both high and low extreme values of their probability distributions (generally corresponding to the 10$^{th}$ and 90$^{th}$ percentile), and the outputs are

measured. When one variable is set to the two extreme values of its probability distribution function, all the others are fixed to their median values. The absolute value of the difference between these two outputs, called "*swing*", is the measure of the EDP sensitivity to the selected input parameter. Finally, the input parameters are ranked according to their swings so that the larger swing belongs to the variable producing the most significant uncertainty (Figure 4.1). An extensive review of the Tornado diagram method can be found in Porter et al. (2002) and Lee and Mosalam (2005), and applications of this method are in Binici and Mosalam (2007) and Talaat and Mosalam (2007).

Since this work aims to evaluate the variability of the seismic demand with respect to the application of different selection and scaling criteria of ground motion records, only uncertainties in earthquake action are considered. More specifically, the selected input variables are the Intensity Measure (IM), $S_a(T^*)$, and the Ground Motion (GM) profile. Based on the original assumptions of the Tornado diagram analysis, all records should be scaled to the IM value corresponding to the median value of its probability distribution function, that is $S_a(T^*)$, corresponding to 50% probability of exceedance in 50 years. This probability of exceedance corresponds to earthquakes characterized by a return period $T_R$ of 72 years. In order to use records representing the Ultimate Limit State (ULS) requirements (with $T_R$ = 475 years), the probability of exceedance is fixed to 50% according to the Tornado analysis assumptions, but the exposure period is varied. Assuming a Poisson recurrence law for the mean annual exceedance rate λ, the probability of exceedance P of a given intensity measure over an exposure time *t* is expressed by Eq. 4.1, where $\lambda = 1/T_R$:

$$P = 1 - e^{-\lambda t} \tag{4.1}$$

The exposure period *t* corresponding to a return period of 475 years is equal to 330 years. All records used for the Tornado analysis are then scaled to $S_a(T^*)$ corresponding to the median exceedance probability of 50% in 330 years (equivalent to an exceedance probability of 10% in 50 years). The variation of the GM keeping the IM fixed is obtained by using records scaled to the same IM = $S_a(T^*)$. The Tornado diagram bar corresponding to the variation of the GM profile is obtained from the 10% and 90% fractiles of the EDPs derived from a record to record analysis. The scaled records considered in this work are those belonging to Comb.1, Comb.2 and Comb. 3.

The seismic demand variability provided by the IM variation is measured by fixing the GM variable to its median value and varying $S_a(T^*)$ to the 10$^{th}$ and 90$^{th}$ percentile of its probability distribution fuction. More specifically, since the Tornado diagram analysis requires that the uncertain input variables vary one to one, the GM variable has to be fixed to its median value. For this reason, only one record is considered, that is the ground motion producing the median EDP from the record to record analysis. This record is then scaled to the $S_a(T^*)$ values corresponding to non-exceedance probabilities of 10% and 90% in 330 years. The return periods corresponding to these non-exceedance probabilities estimated with Eq. 4.1 are respectively 143 and 3107 years. The 10$^{th}$ and 90$^{th}$ percentile of $S_a(T^*)$ is obtained through a lognormal interpolation of the spectral values obtained by the PSHA, which provides, for the selected specific-site, uniform hazard spectra for nine hazard levels with return periods of 30, 50, 72, 101, 140, 201, 475, 975 and 2475 years. Figure 4.2 shows the Lognormal Probability Distribution Function PDF (on the right) and the Cumulative Distribution Function CDF (on the left) of $S_a(T^*)$ corresponding to Structure 1.

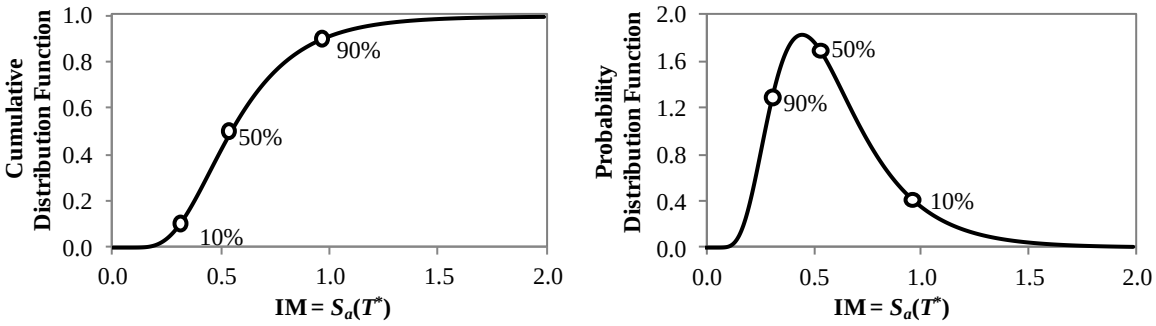

**Figure 4.2.** Lognormal Cumulative (on the left) and Probability (on the right) Distribution Functions of $S_a(T^*)$ values of Structure 1 for an exposure period of 330 years.

## 5. RESULTS AND DISCUSSION

The Tornado diagrams obtained for each structure and record combination are summarized in Figure 5.1. Each of the ten plots refers to a different structure and contains three Tornado diagrams carried out by considering the sets of records selected according to the minimization of the scale factor (Comb. 1) and the spectrum-compatibility (Comb. 2- Comb. 3) criteria. All Tornado diagrams define the demand variability with respect to the IM = $S_a(T^*)$ and the GM profile. The Tornado diagrams show that the demand variability produced by the application of different seismic inputs (GM) is almost always lower than that produced by the variation of the intensity measure (IM).

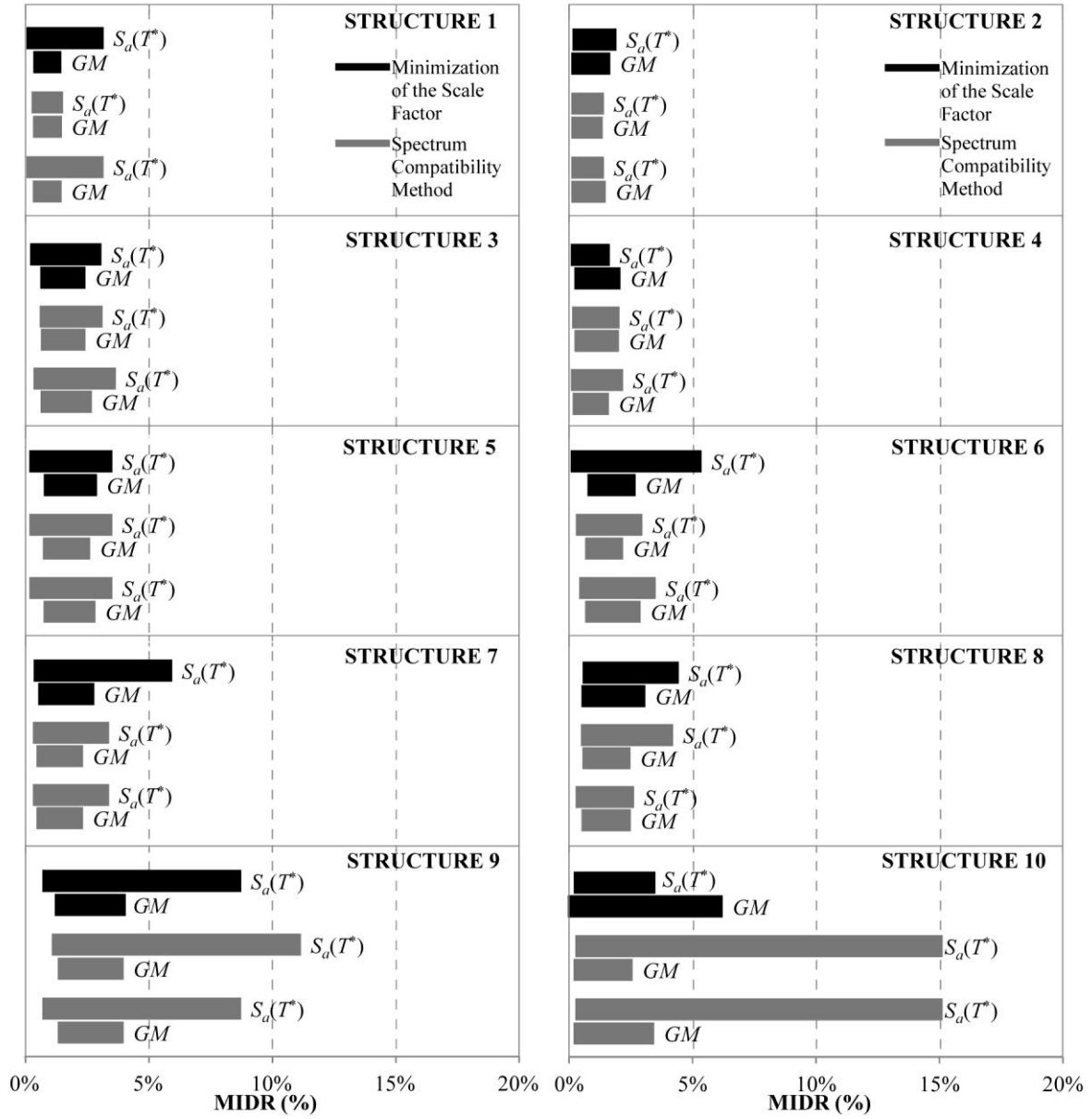


**Figure 5.1.** Tornado diagrams obtained subjecting each of the 10 analyzed structures to three different sets of 20 ground motion records scaled on $S_a(T^*)$ and using as input variables the GM profile and IM = $S_a(T^*)$.

In order to evaluate the selection and scaling criterion producing the smallest uncertainty in the seismic demand, only the variability provided by the GM variation is considered. Figure 5.2 summarizes in a single graph all the EDP variabilities generated by the variation of the GM profile derived from the 30 Tornado diagrams represented in Figure 5.1. The variability of the seismic demand increases significantly with the increasing of the structural complexity and irregularity. More specifically, for very regular structures (as Structure 1), the two analyzed GMSM methods provide very similar variability, while for complex and irregular structures the adopted spectrum-compatibility criterion produces the smaller EDP variability. This occurs because the spectrum-compatibility method requires that the mean spectrum obtained with the selected ground motions is similar to the target spectrum obtained by the PSHA in a wide range of periods. When the criterion based on the minimization of the scale factor is used, the selected spectra can be different from each other, except from the scaling point. If a structure is irregular, its dynamic behaviour is affected by a large range of frequencies, in particular when the structure goes into the non-linear region as in this case the structural period undergoes large oscillations during the analysis.

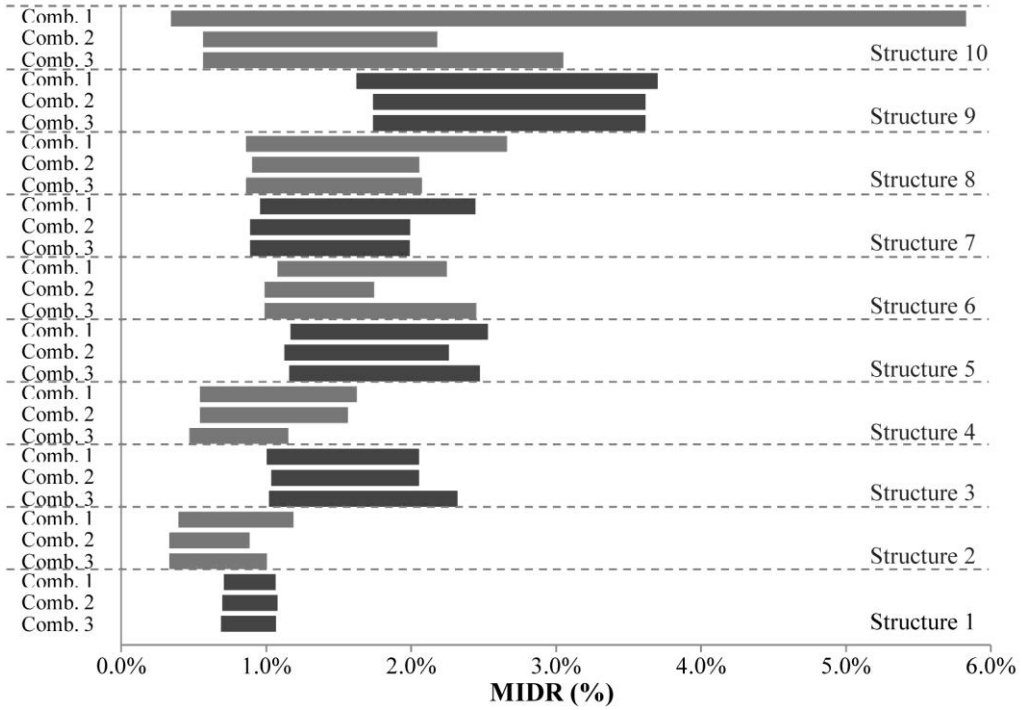


**Figure 5.2.** Tornado diagrams obtained for the 10 structures using as input variable the GM profile; for each structure, three Tornado diagrams are shown: in Comb. 1, records are selected minimizing the scale factor, while in Comb. 2 - 3 by using the spectrum-compatibility criterion.

The relative influence of the structural irregularity on the EDP variability generated by the two considered GMSM methods can be quantified by relating the variability produced by the different record combinations with a parameter summarizing the irregularity degree of each structure. One of the numerous parameters providing information on structural behavior is the 1$^{st}$ mode participation factor, able to capture especially the vertical irregularity of the structure. Figure 5.3 shows the correlations between the EDP variability due to the variation in GM profile derived from the ten analyzed structures and the corresponding 1$^{st}$ mode participation factors $\Gamma_1$, whose values are shown in Table 2.2. The three different plots refer respectively to the three ground motion combinations (Comb.1, Comb. 2 and Comb. 3) applied to each RC structure. The measure of the correlation between the two parameters is estimated through the determination coefficients $R^2$, whose values between 0 and 1 reveal how closely a value predicted through a trendline ($Y_{pi}$) corresponds to the actual data ($Y_i$):

$$R^2 = \frac{\sum_i^n \left( Y_{pi} - Y_m \right)^2}{\sum_i^n \left( Y_i - Y_m \right)^2} \tag{5.1}$$

where $Y_m$ = mean value and $n$ = total number of points.

The data are fitted through linear and polynomial regression lines whose equations are respectively $y = ax+c$ and $y = ax+bx^2$, where $a$, $b$ and $c$ are constant coefficients.

For all considered sets of records, the increase of the modal participation factor corresponds to a general increment of the variability of the structural demand. However, the trends of the linear and polynomial regression lines show that spectrum-compatible records (Comb. 2 and Comb. 3) produce EDP uncertainties less sensitive to the structural irregularities than records selected minimizing the scale factors (Comb. 1).

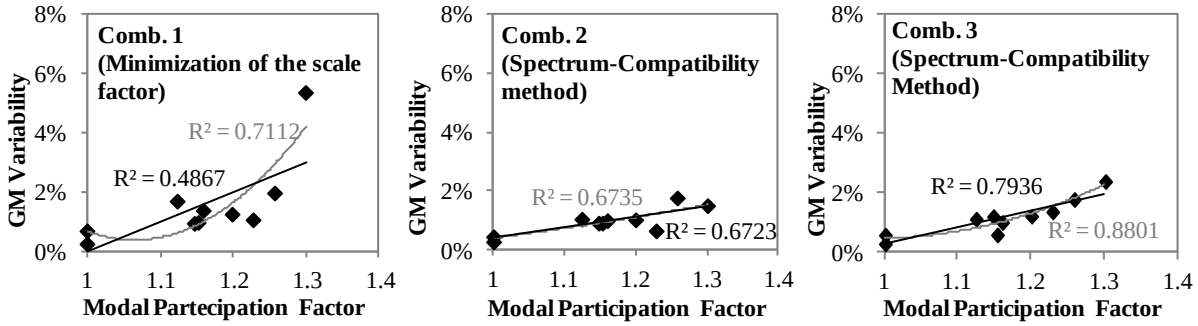


**Figure 5.3.** Correlations between the seismic demand variability derived from the 10 analyzed structures due to the variation in GM profile and the corresponding first mode participation factors; in black and grey are represented respectively the linear and polynomial regression lines.

## 5. CONCLUSIONS

In this work the sensitivity of ten RC structures analyzed by NLTHA to several GMSM methods is investigated. For this reason a first-order sensitivity analysis, called *Tornado diagram analysis*, is used. The considered random input variables are the Intensity Measure (IM) and the Ground Motion (GM) profile, while the EDP is the MIDR. Each structure is subjected to three different sets of 20 ground motion records scaled to the target spectral acceleration $S_a(T^*)$ and selected according to the minimization of the scale factor (Comb. 1) and the spectrum-compatibility (Comb. 2 – Comb. 3) criteria. The application of the sensitivity analysis to the different structure and record combinations provided the results summarized in the following points:

1. The EDP variability produced by the application of different records (GM) is lower than the variability induced by the variation of the intensity measure (IM).

2. The variability of the structural demand induced by the variation of the GM profile intensifies significantly with the increasing of the structural complexity and irregularity.

3. The EDP variability provided by very regular structures subjected to records selected according to the minimization of the scale factor and the spectrum-compatibility criteria are very similar.

4. The seismic demand uncertainty of irregular structures is smaller if they are subjected to ground motion records selected according to the spectrum-compatibility criterion. The trends of the linear and polynomial regression lines obtained correlating, for each record combination, the EDP

variability with the 1st mode participation factor, show that spectrum-compatible records produce EDP uncertainties less sensitive to the structural irregularities than records selected minimizing the scale factors.

**AKCNOWLEDGEMENT**

The authors would like to acknowledge the financial support from the ReLUIS program of the Italian Civil Protection Agency (DPC), task 1.1.2, contract n. 823, 24/09/2009.

**REFERENCES**

Bazzurro, P. and Cornell, C.A. (1999). Disaggregation of seismic hazard. *Bulletin of the Seismological Society of America* **89:2**, 501-520.

Beyer, K. and Bommer, J.J. (2006). Relationships between median values and between aleatory variabilities for different definitions of the horizontal component of motion. *Bulletin of the Seismological Society of America*, **96:4A**, 1512–1522.

Binici, B. and Mosalam, K.M. (2007). Analysis of Reinforced Concrete Columns Retrofitted with Fiber Reinforced Polymer Lamina. *Composites Part B: Engineering*, **38:2**, 265-276.

Cantagallo, C., Camata, G., Spacone, E. and Corotis, R. (2012). The Variability of Deformation Demand with Ground Motion Intensity. *Probabilistic Engineering Mechanics*, **28**, 59-65.

Eschenbach, T.G. (1992). Spiderplots versus Tornado Diagrams for Sensitivity Analysis. *Decision and Risk Analysis*, **22:6**, pp. 40-46.

European Strong-motion Database (ESD). *http://www.isesd.cv.ic.ac.uk/ESD/frameset.htm*.

Faggella, M., Barbosa, A.R., Conte, J.P., Spacone, E and Restrepo, J.I. (2012). Probabilistic Seismic Response Analysis of a 3-D Reinforced Concrete Building. *ASCE Journal of Structural Engineering*, submitted.

ITalian ACcelerometric Archive (ITACA). *http://itaca.mi.ingv.it/ItacaNet/*.

Kent, D. C. and Park, R. (1971). Flexural members with confined concrete, *Journal of the Structural Division*, **97:7**, 1969–1990.

Lee, T.H. and Mosalam, K.M. (2005). Seismic Demand Sensitivity of Reinforced Concrete Shear-Wall Building Using FOSM Method. *Earthquake Engineering and Structural Dynamics*, **34:14**, 1719-1736.

López, A. and Hernández, J. J. (2004). Structural Design for Multicomponent Seismic Motion, Vancouver, B.C., Canada, in *Proceedings, 13th World Conference on Earthquake Engineering*, paper 2171.

Menegotto, M. and Pinto, P. E. (1973). Method of analysis for cyclically loaded reinforced concrete plane frames including changes in geometry and nonelastic behavior of elements under combined normal force and bending. Zurich, in *Proceedings, IABSE Symposium on Resistance and Ultimate Deformability of Structures Acted on by Well Defined Repeated Loads*, pp. 112-123.

MIDAS/Gen, ver. 7.2.1 (2007), *http://www.cspfea.net/midas_gen.php*.

Penzien, J. and Watabe, M. (1975). Characteristics of 3-dimensional earthquake ground motion. *Earthquake. Engineering and Structural Dynamics* **3:4**, 365-374.

Porter, K. A., Beck, J. L. and Shaikhutdinov, R. V. (2002). Sensitivity of building loss estimates to major uncertain variables. *Earthquake Spectra*, **18:4**, 719–743.

Spacone, E., Filippou, F. C. and Taucer, F. (1996). Fiber Beam-Column Model for Nonlinear Analysis of R/C Frames: I. Formulation. *Earthquake Engineering and Structural Dynamics* **25:7**, 711-725.

Spallarossa, D. and Barani, S. (2007). Progetto DPC-INGV S1, Deliverable D14, *http://esse1.mi.ingv.it/d14.html*.

Talaat, M.M. and Mosalam K.M. (2010). Computational modeling of progressive collapse in reinforced concrete frame structures, *PEER-2007/10, Pacific Earthquake Engineering Research Center* (PEER), University of California, Berkeley.

UNI EN 1998-1:2005, *Eurocode 8: Design of structures for earthquake resistance* - Part 1: General rules, seismic actions and rules for buildings, EN1998-1-1, Brussels, 2004.